Journal of Global Positioning Systems (2005)
Vol. 4, No. 1-2: 65-75

Journal of Global Positioning Systems
2005

Wide-lane Assisted Long Baseline High Precision Kinematic Positioning by GNSS

Hiroshi Isshiki

IMA (Institute of Mathematical Analysis), B507, 3-11, Nishiyamadai 6-chome, Osaka-Sayama, Osaka 589-0022, Japan
e-mail: isshiki@dab.hi-ho.ne.jp Tel: +81-072-367-7139; Fax: +81-072-367-7139

Received: 8 November 2004 / Accepted: 13 July 2005

Abstract. In the previous report (Isshiki, 2004b), theory and algorithm of a new dual frequency long baseline kinematic positioning method were discussed. In the theory, the wide-lane coordinates are used as a constraint for obtaining the correct L1 ambiguities by solving the ionosphere free equations. The effectiveness was verified by some numerical examples. A precise positioning for baseline of several hundred kilometeres are possible. In the present report, the effect of epoch interval and observation length is investigated by numerical calculations. The relationship between the positioning error and the baseline length is also discussed. Furthermore, an algorithm for the real time application is shown.

Key words: wide-lane, long baseline, high precision, kinematic positioning, GNSS

1 Introduction

In the previous report (Isshiki, 2004b), new theory and algorithm for dual frequency long baseline kinematic positioning were discussed. The theory is based on the facts that the initial phase ambiguities of the wide-lane combinations can be obtained correctly irrespective of the baseline length by using HMW (Hatch-Melbourne-Wübbena) combinations (Hatch, 1982; Melbourne, 1985; Wübbena, 1985), the slowly varying part of the ionospheric delays can be estimated with an appropriate accuracy from an external information source such as IONEX (Hugeltobler *et al.*, 2001), and the rapidly varying part can be obtained correctly by using the geometry-free combinations. Specifically, the coordinates of the observation receiver can be obtained rather precisely by solving the wide-lane combinations by using the above-mentioned ambiguities and the ionospheric delays. And the coordinates are used to impose an constraint to the least squares solution of the ionosphere free combinations. This corresponds to the constraint in the case of static positioning where the coordinates are constant.

In the previous report, the validity of the new solution was verified by using data with the epoch interval of thirty seconds downloaded from the homepage of GSI (Geographical Survey Institute, http://terras.gsi.go.jp /inet_NEW/). This new solution makes kinematic positioning for the baseline length of several hundred kilometers possible.

In the present report, the effects of the number of the epoch and observation length are discussed by using data with the epoch interval of one second which can't be downloaded directly from the above-mentioned homepage. The relationship between the baseline length and the positioning error is also investigated. And the algorithm for the real time processing is discussed too.

2 Theory

Double difference observation equations of the pseudo range $P_{\kappa\alpha}^{\ i}(t)$ and the phase range $\Phi_{\kappa\alpha}^{\ i}(t)$ are given as (Isshiki, 2003a-c, 2004a; Hugeltobler et al., 2001)

$$P_{\kappa\alpha\beta}^{\ i\,j} = \rho_{\alpha\beta}^{i\,j} + \left(\frac{f_1}{f_\kappa}\right)^2 I_{\alpha\beta}^{i\,j} + T_{\alpha\beta}^{i\,j} + e_{\kappa\alpha\beta}^{\ i\,j}, \tag{1a}$$

$$\Phi_{\kappa\alpha\beta}^{\ i\,j} = \rho_{\alpha\beta}^{i\,j} - \left(\frac{f_1}{f_\kappa}\right)^2 I_{\alpha\beta}^{i\,j} + T_{\alpha\beta}^{i\,j} + \lambda_\kappa N_{\kappa\alpha\beta}^{\ i\,j} + \varepsilon_{\kappa\alpha\beta}^{\ i\,j}, \tag{1b}$$

where

$$(\bullet)_{\alpha\beta}^{i} = (\bullet)_{\alpha}^{i} - (\bullet)_{\beta}^{i},$$

$$(\bullet)^{ij}_{\alpha} = (\bullet)^{i}_{\alpha} - (\bullet)^{j}_{\alpha}\,, \tag{2}$$

$$(\bullet)^{ij}_{\alpha\beta} = (\bullet)^{i}_{\alpha\beta} - (\bullet)^{j}_{\alpha\beta} = (\bullet)^{ij}_{\alpha} - (\bullet)^{ij}_{\beta}\,.$$

The subscripts $\kappa = 1, 2$ refer to the L1 and L2 signals, and the superscript i and the subscript α refer to the satellite and the receiver. f_κ denotes the frequency of κ signal. $I^{ij}_{\alpha\beta}$ and $T^{ij}_{\alpha\beta}$ are the ionospheric and tropospheric delays. $N_{\kappa}{}^{ij}_{\alpha\beta}$ is the initial phase ambiguity.

The initial phase ambiguities of the wide-lane combination can be determined easily for each combination of the satellite and receiver by using HMW (Hatch-Melbourne-Wübbena) combination irrespective of the baseline length. Specifically, if HMW combination:

$$N_{W\kappa\lambda}{}^{ij}_{\alpha\beta} \equiv N_{\kappa}{}^{ij}_{\alpha\beta} - N_{\lambda}{}^{ij}_{\alpha\beta}$$

$$= \frac{\Phi_{\kappa}{}^{ij}_{\alpha\beta}(t)}{\lambda_\kappa} - \frac{\Phi_{\lambda}{}^{ij}_{\alpha\beta}(t)}{\lambda_\lambda} - \frac{f_\kappa - f_\lambda}{f_\kappa + f_\lambda}\left(\frac{P_{\kappa}{}^{ij}_{\alpha\beta}(t)}{\lambda_\kappa} + \frac{P_{\lambda}{}^{ij}_{\alpha\beta}(t)}{\lambda_\lambda}\right) \tag{3}$$

is used, the wide-lane ambiguity $N_{W\kappa\lambda}{}^{ij}_{\alpha\beta}$ is obtained, where λ_κ and λ_λ refer to the wave lengths of κ and λ signals (→ Eq. (10)). This equation uses not only the phase ranges but also pseudo ranges, but the coefficient multiplied to the pseudo ranges is small. So, the noise in the pseudo range is suppressed.

If the geometry free combination $\Phi_{G\kappa\lambda}{}^{ij}_{\alpha\beta}(t)$:

$$\Phi_{G\kappa\lambda}{}^{ij}_{\alpha\beta}(t) \equiv \Phi_{\kappa}{}^{ij}_{\alpha\beta}(t) - \Phi_{W\kappa\lambda}{}^{ij}_{\alpha\beta}(t)$$

$$= -\frac{f_1}{f_\kappa}\left(\frac{f_1}{f_\kappa} + \frac{f_1}{f_\lambda}\right) I^{ij}_{\alpha\beta}(t) + \lambda_\kappa N_{\kappa}{}^{ij}_{\alpha\beta} - \lambda_{W\kappa\lambda} N_{W\kappa\lambda}{}^{ij}_{\alpha\beta} \tag{4}$$

is used, the rapidly varying part of the ionospheric delay can be determined correctly even when the initial phase ambiguity is unknown (Isshiki, 2003c, 2004a). Hence, if the slowly varying part is estimated by external information such as IONEX, a fairly correct estimate of the ionospheric delay may be possible.

The ionospheric delay $I^{ij}_{\alpha\beta}(t)$ is then decomposed into the slowly varying component $\bar{I}^{ij}_{\alpha\beta}$ and the rapidly varying component $\tilde{I}^{ij}_{\alpha\beta}(t)$:

$$I^{ij}_{\alpha\beta}(t) = \bar{I}^{ij}_{\alpha\beta} + \tilde{I}^{ij}_{\alpha\beta}(t)\,, \tag{5}$$

$$\bar{I}^{ij}_{\alpha\beta} = \frac{1}{T}\int_0^T I^{ij}_{\alpha\beta}(t)dt\,, \tag{6a}$$

$$\tilde{I}^{ij}_{\alpha\beta}(t) = I^{ij}_{\alpha\beta}(t) - \bar{I}^{ij}_{\alpha\beta}\,, \tag{6b}$$

where T is the measuring time. If $N_{\kappa}{}^{ij}_{\alpha\beta}$ is known, from Eqs. (4) and (5)

$$\bar{I}^{ij}_{\alpha\beta} = \left\{\begin{array}{l} -\dfrac{1}{T}\displaystyle\int_0^T\left[\Phi_{\kappa}{}^{ij}_{\alpha\beta}(t) - \Phi_{W\kappa\lambda}{}^{ij}_{\alpha\beta}(t)\right]dt \\ +\lambda_\kappa N_{\kappa}{}^{ij}_{\alpha\beta} - \lambda_{W\kappa\lambda} N_{W\kappa\lambda}{}^{ij}_{\alpha\beta} \end{array}\right\} \Bigg/ \left\{\frac{f_1}{f_\kappa}\left(\frac{f_1}{f_\kappa} + \frac{f_1}{f_\lambda}\right)\right\}. \tag{7}$$

The rapidly varying part is written as

$$\tilde{I}^{ij}_{\alpha\beta}(t) = \left\{\begin{array}{l} -\left[\Phi_{\kappa}{}^{ij}_{\alpha\beta}(t) - \Phi_{W\kappa\lambda}{}^{ij}_{\alpha\beta}(t)\right] \\ +\dfrac{1}{T}\displaystyle\int_0^T\left[\Phi_{\kappa}{}^{ij}_{\alpha\beta}(t) - \Phi_{W\kappa\lambda}{}^{ij}_{\alpha\beta}(t)\right]dt \end{array}\right\} \Bigg/ \left\{\frac{f_1}{f_\kappa}\left(\frac{f_1}{f_\kappa} + \frac{f_1}{f_\lambda}\right)\right\}. \tag{8}$$

Since Eq. (8) uses only the phase ranges, the rapidly varying component $\tilde{I}^{ij}_{\alpha\beta}(t)$ can be estimated very precisely.

For the estimation of the mean component $\bar{I}^{ij}_{\alpha\beta}$, the use of the pseudo range or IONEX may be considered. In thecase of using IONEX, the measuring time T should be longer than the periods of the rapidly varying components. And much attention should also be paid to the reliability of the external information such as IONEX.

If the kinematic positioning using wide-lane combination is conducted together with the correctly obtained ambiguities and the reasonably estimated ionospheric delays, the receiver coordinates may be obtained rather precisely.

The WL (wide-lane) combination $\Phi_{W\kappa\lambda}{}^{ij}_{\alpha\beta}(t)$ is given as

$$\Phi_{W\kappa\lambda}{}^{ij}_{\alpha\beta}(t) \equiv \frac{\lambda_{W\kappa\lambda}}{\lambda_\kappa}\Phi_{\kappa}{}^{ij}_{\alpha\beta}(t) - \frac{\lambda_{W\kappa\lambda}}{\lambda_\lambda}\Phi_{\lambda}{}^{ij}_{\alpha\beta}(t)$$

$$= \rho^{ij}_{\alpha\beta} - \left[\frac{\lambda_{W\kappa\lambda}}{\lambda_\kappa}\left(\frac{f_1}{f_\kappa}\right)^2 - \frac{\lambda_{W\kappa\lambda}}{\lambda_\lambda}\left(\frac{f_1}{f_\lambda}\right)^2\right] I^{ij}_{\alpha\beta}$$

$$+ \lambda_{W\kappa\lambda}\left(N_{\kappa}{}^{ij}_{\alpha\beta} - N_{\lambda}{}^{ij}_{\alpha\beta}\right) + T^{ij}_{\alpha\beta} + \varepsilon_{W\kappa\lambda}{}^{ij}_{\alpha\beta}$$

$$= \rho^{ij}_{\alpha\beta} + \frac{f_1^2}{f_\kappa f_\lambda} I^{ij}_{\alpha\beta} + \lambda_{W\kappa\lambda} N_{W\kappa\lambda}{}^{ij}_{\alpha\beta} + T^{ij}_{\alpha\beta} + \varepsilon_{W\kappa\lambda}{}^{ij}_{\alpha\beta}\,, \tag{9}$$

where $f_{W\kappa\lambda}$ and $\lambda_{W\kappa\lambda}$ are the virtual frequency and the wave length of the wide-lane signal and given as

$$\frac{f_{W\kappa\lambda}}{c} = \frac{f_\kappa - f_\lambda}{c} = \frac{1}{\lambda_\kappa} - \frac{1}{\lambda_\lambda}\,, \tag{10a}$$

$$\lambda_{W\kappa\lambda} = \frac{c}{f_\kappa - f_\lambda} = 1 \Big/ \left(\frac{1}{\lambda_\kappa} - \frac{1}{\lambda_\lambda} \right). \tag{10b}$$

When the above-mentioned receiver coordinates of the observation point is substituted into the IF (Ionosphere free) combination $\Phi_{I\kappa\lambda\,\alpha\beta}^{\ ij}(t)$:

$$\Phi_{I\kappa\lambda\,\alpha\beta}^{\ ij}(t)$$

$$\equiv \frac{1}{2}\left[\frac{\lambda_{N\kappa\lambda} + \lambda_{W\kappa\lambda}}{\lambda_\kappa} \Phi_{\kappa\alpha\beta}^{\ ij}(t) + \frac{\lambda_{N\kappa\lambda} - \lambda_{W\kappa\lambda}}{\lambda_\lambda} \Phi_{\lambda\alpha\beta}^{\ ij}(t) \right]$$

$$= \rho_{\alpha\beta}^{ij} + \left(\lambda_{N\kappa\lambda} N_{\kappa\alpha\beta}^{\ ij} + \frac{c f_\lambda}{f_\kappa^{\ 2} - f_\lambda^{\ 2}} N_{W\kappa\lambda\,\alpha\beta}^{\ ij} \right) + T_{\alpha\beta}^{ij} + \varepsilon_{I\kappa\lambda\,\alpha\beta}^{\ ij} \tag{11}$$

a close approximation of the initial phase ambiguity $N_{\kappa\alpha\beta}^{\ ij}$ of the L1 signal is obtained. In the IF combination, the ionospheric delay $I_{\alpha\beta}^{ij}(t)$ is eliminated. The L1 ambiguities are rounded to integers. An integer grid is made around a point consisting of the set of the above-mentioned L1 integer ambiguities. A point on the grid which makes the product of the residuals of the least squares solution of the IF combinations and the distance between the above-mentioned coordinates obtained by the LW combinations and those by the IF combinations minimum is searched on the integer grids. As the result, very precise L1 ambiguities and receiver coordinates for the baseline length of several hundred kilometers are obtained, if the sufficient length is secured for observation time.

In Fig. 4, a flow of algorithm in case of real-time processing is shown. For offline processing, the repetition of calculation for each epoch is not necessary, and the averaging should be conducted in the whole epochs.

3 Observation data

Observation data for fixed stations used in the following numerical examples are shown in Tables 1a and 1b. They are obtained by GEONET operated by GSI (Geographical Survey Institute) and are similar to those used in the previous report (Isshiki, 2004b). The date of the observation data is June 4, 2004. In the previous report, the epoch interval was thirty seconds alone, but, in the present report, data of one second in epoch interval are also used. The thirty second data were downloaded from the homepage of GSI (http://terras.gsi.go.jp /inet_NEW/). The one second data can't be downloaded from the homepage. They were obtained from a source different from GSI. The both data are available for the stations with * in Tables 1a and 1b, and only the thirty second data for other stations. The observation data between GPS time 09:00:00 and 11:00:00 were used for the numerical calculations. The station coordinates in Table 1a are downloaded from the above-mentioned homepage, and the accuracy is very high. The baseline lengths are very close to those shown in Table 1b of the previous report, but the difference of baseline length between Sapporo and Hakodate is a little bit big. In the following calculations, the temporary data are used for the orbits and the ionospheric delays instead of the final data. For reference, some comparisons are shown on the difference between the results obtained by the temporary data and those by the final data.

4 Effects of epoch interval and observation length

4.1 Effects of epoch interval

First. the effects of the epoch interval are studied where the observation length is two hours. The results for SpprMrrn baseline (72209.202 m) are shown below. Table 2a shows the correct values of $N_{W12\,\alpha\beta}^{\ \ ij}$ and $N_{1\alpha\beta}^{\ ij}$.

Tab. 1a Stations and coordinates (GEONET: 04.06.04)

Stn Name	Stn.ID	Abribiation	$x \quad (m)$	$y \quad (m)$	$z \quad (m)$
Sapporo*	950128	Sppr	-3647450.0190	2923169.1696	4325315.2989
Chitose	960523	Chts	-3665179.0969	2925131.3183	4309263.7688
Tomakomai*	950136	Tmkm	-3681909.6939	2918009.3245	4299470.4964
Muroran*	940018	Mrrn	-3664512.7967	2973568.1063	4276499.5476
Sawara*	960528	Sawr	-3664617.9412	3002995.5330	4255789.3878
Hakodate*	940022	Hkdm	-3685967.8639	3011795.3488	4231283.2112
Iwaizumi*	950164	Iwa2	-3853718.7701	3032158.1371	4065250.0274
Kesennuma	950172	Ksnm	-3893613.1909	3089073.8262	3983982.4123
Kitaibaraki	950214	Ktib	-3959969.0560	3234979.5092	3799716.9881
Ichikawa	93023	Ichk	-3967874.2600	3340981.7196	3699025.1130

Tab. 1b Relative coordinates (dx, dy, dz) between stations and baseline length dr (GEONET: 04.06.04)

BL Name	dx (m)	dy (m)	dz (m)	dr (m)
SpprChts	-17729.0779	1962.1487	-16051.5301	23996.2882
HkdmSawr*	-21349.9227	8799.8158	-24506.1766	33672.0752
SpprTmkm*	-34459.6749	-5159.8451	-25844.8025	43382.5658
TmkmMrrn*	17396.8972	55558.7818	-22970.9488	62586.6979
SpprMrrn*	-17062.7777	50398.9367	-48815.7513	72209.2015
SpprSawr*	-17167.9222	79826.3634	-69525.9111	107241.9608
SpprHkdm*	-38517.8449	88626.1792	-94032.0877	134834.1853
HkdmIwa2*	-167750.9062	20362.7883	-166033.1838	236900.8818
MrrnIwa2*	-189205.9734	-58590.0308	211249.5202	289582.5476
SpprIwa2*	-206268.7511	108988.9675	-260065.2715	349369.9159
SpprKsnm	-246163.1719	165904.6566	-341332.8866	452359.1513
SpprKtib	-312519.0370	311810.3396	-525598.3108	686401.7925
SpprIchk	-320424.2410	417812.5500	-626290.1859	818216.6083

${N_{W12}}_{\alpha\beta}^{ij}$ are obtained by HMW combinations and ${N_1}_{\alpha\beta}^{ij}$ by the static positioning of the ionosphere free combinations. Table 2b shows a relationship between the epoch interval and the L1 ambiguity ${N_1}_{\alpha\beta}^{ij}$ estimated by the present method. For example, the epoch interval 90 sec corresponds to having 80 data in 2 hours. The same results are obtained irrespective of the epoch interval. The results of the estimated baseline length are shown in Table 2c. The values in Tables 2a and 2b show very small difference, but they give the almost same positioning results as shown in Figs. 1a and 1b. So, the difference may be considered allowable. From the above-mentioned results, if the observation length is equal, the effects of the epoch interval may be small. This may correspond to the fact that the number of the observation equations per unknown does not increase in case of the kinematic positioning.

Tab. 2a Correct double differences DDNW and DDN1 of LW and L1 ambiguities (SpprMrrn, 04.06.04; 09:00:00-11:00:00; IGR12735, ESAG1560)

	((09)-(05))	((14)-(05))	((22)-(05))	((30)-(05))
DDNW	5174360	-2110139	1387665	-2380484
DDN1	23350963	-10737766	6488635	-13439396

Tab. 2b Estimated double difference DDN1 of L1 ambiguity (Obt1Ion1: precise orbit, IONEX; measuring time: 2 hours)

1 epoch	((09)-(05))	((14)-(05))	((22)-(05))	((30)-(05))
90 sec	23350963	-10737767	6488634	-13439396
60 sec	23350963	-10737767	6488634	-13439396
45 sec	23350963	-10737767	6488634	-13439396
30 sec	23350963	-10737767	6488634	-13439396
15 sec	23350963	-10737767	6488634	-13439396

Tab. 2c Estimated baseline length

1 epoch	Avg of BL by LI (m)	Sgm of BL by LI (m)	Avg of BL by LW (m)	Sgm of BL by LW (m)
90 sec	72209.219	0.014	72209.267	0.014
60 sec	72209.216	0.013	72209.264	0.014
45 sec	72209.215	0.014	72209.264	0.014
30 sec	72209.215	0.014	72209.263	0.014
15 sec	72209.214	0.014	72209.262	0.014

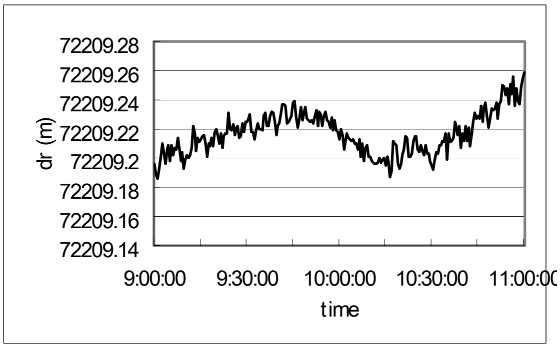

Fig. 1a Baseline length calculated by using L1 ambiguities in Table 2a

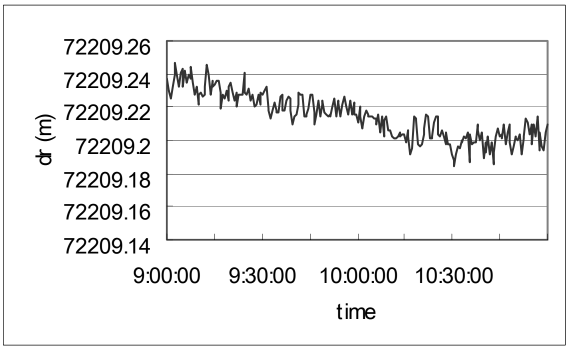

Fig. 1b Baseline length calculated by using L1 ambiguities in Table 2b

Tab. 3a Estimated double difference DDN1 of L1 ambiguity (Obt1Ion1: precise orbit, IONEX; 240 epochs)

Obs. Length	((09)-(05))	((14)-(05))	((22)-(05))	((30)-(05))
20 min	23350965	-10737767	6488633	-13439397
32 min	23350964	-10737766	6488634	-13439396
40 min	23350963	-10737767	6488634	-13439396
60 min	23350963	-10737767	6488634	-13439396
80 min	23350963	-10737767	6488634	-13439396
100 min	23350963	-10737767	6488634	-13439396
120 min	23350963	-10737767	6488634	-13439396

Tab. 3b Estimated baseline length of SpprMrrn (Obt1Ion1: precise orbit, IONEX; 240 epochs)

Obs. Length	Avg of BL by LI (m)	Sgm of BL by LI (m)	Avg of BL by LW (m)	Sgm of BL by LW (m)
20 min	72209.541	0.028	72209.235	0.007
32 min	72209.360	0.022	72209.276	0.008
40 min	72209.228	0.008	72209.280	0.009
60 min	72209.224	0.008	72209.280	0.009
80 min	72209.221	0.011	72209.274	0.012
100 min	72209.217	0.014	72209.265	0.015
120 min	72209.215	0.014	72209.263	0.014

Tab 4 Effects due to accuracy of orbit and ionospheric delay (Temporary File: IGR, ESAG; Final File: IGS, CODG)

	Avg of BL by LI (m)	Sgm of BL by LI (m)	Avg of BL by LW (m)	Sgm of BL by LW (m)
Temp.	72209.215	0.014	72209.263	0.014
Final	72209.215	0.014	72209.280	0.016

4.2 Effects of observation length

Next, the effects of the observation length are studied. The observation length is varied by changing the epoch interval of the 240 epochs. The results are shown in Tables 3a and 3b.

The orbits and ionospheric delays are not the final data (IGS, CODG) but the temporary data (IGR, ESAG). In Table 4 and Fig. 2, the baseline length obtained by using the final data is compared with the case obtained by using the temporary data. The temporary data seem sufficient at least for the baseline SpprMrrn whose baseline length is 72209.202 m .

The results where the orbits are approximated by the broadcast orbits and the ionospheric delays are neglected are shown in Table 5 for reference. The comparison between Tables 3 and 5 suggests that the observation length required for the convergence of the calculation seems shortened.

As another example, a case where the baseline is relatively short is discussed. In applications on land, the short baseline positioning is considered important.

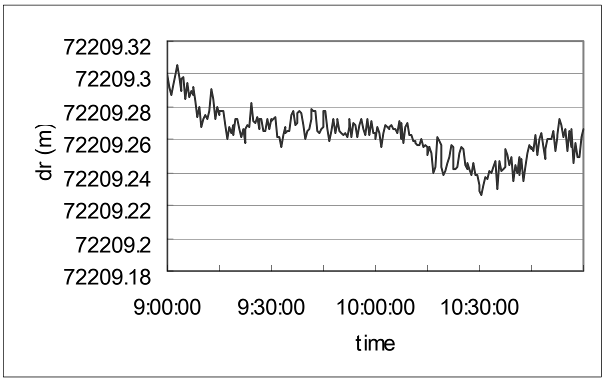

Fig. 2a Baseline length by LW where temporary orbits IGR and ionospheric delay estimates ESAG are used

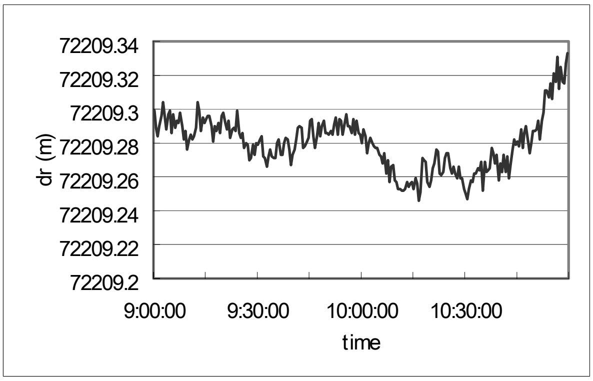

Fig. 2b Baseline length by LW where final orbits IGS and ionospheric delay estimates CODG are used

Tab. 5a Estimated double difference DDN1 of L1 ambiguity (Obt0Ion0: broadcast orbit, IONEX not used; 240 epochs)

Obs. Length	((09)-(05))	((14)-(05))	((22)-(05))	((30)-(05))
20 min	23350961	-10737767	6488635	-13439394
32 min	23350962	-10737768	6488634	-13439395
40 min	23350962	-10737768	6488634	-13439395
60 min	23350963	-10737767	6488634	-13439396
80 min	23350963	-10737767	6488634	-13439396
100 min	23350963	-10737767	6488634	-13439396
120 min	23350963	-10737767	6488634	-13439396

Tab. 5b Estimated baseline length of SpprMrrn (Obt0Ion0: broadcast orbit, IONEX not used; 240 epochs)

Obs. Length	Avg of BL by LI	Sgm of BL by LI	Avg of BL by LW	Sgm of BL by LW
20 min	72208.886	0.018	72209.304	0.008
32 min	72209.058	0.008	72209.342	0.010
40 min	72209.056	0.008	72209.344	0.011
60 min	72209.230	0.010	72209.345	0.010
80 min	72209.226	0.012	72209.338	0.015
100 min	72209.222	0.015	72209.328	0.017
120 min	72209.218	0.016	72209.328	0.017

Tab. 6a Correct double difference DDNW and DDN1 of LW and L1 ambiguities
(SpprTmkm, 04.06.04; 09:00:00-11:00:00; IGR12735, ESAG1560)

	((09)-(05))	((14)-(05))	((22)-(05))	((30)-(05))
DDNW	5228643	-1292258	2607851	-2630956
DDN1	24045828	-6856447	12167118	-13860004

Tab. 6b Estimated double difference DDN1 of L1 ambiguity
(Obt1Ion1: precise orbit, IONEX; 240 epochs)

Obs. Length	((09)-(05))	((14)-(05))	((22)-(05))	((30)-(05))
16 min	24045828	-6856447	12167118	-13860004
20 min	24045828	-6856447	12167118	-13860004
32 min	24045828	-6856447	12167118	-13860004
40 min	24045828	-6856447	12167118	-13860004
60 min	24045828	-6856447	12167118	-13860004
120 min	24045828	-6856447	12167118	-13860004

Tab. 6c Estimated baseline length of SpprTmkm
(Obt1Ion1: precise orbit, IONEX; 240 epochs)

Obs. length	Avg of BL by LI (m)	Sgm of BL by LI (m)	Avg of BL by LW (m)	Sgm of BL by LW (m)
16 min	43382.572	0.007	43382.558	0.007
20 min	43382.571	0.006	43382.561	0.007
32 min	43382.571	0.007	43382.563	0.010
40 min	43382.571	0.006	43382.566	0.011
60 min	43382.572	0.007	43382.574	0.013
120 min	43382.570	0.009	43382.588	0.023

Tab. 7a Estimated double difference DDN1 of L1 ambiguity
(Obt0Ion0: broadcast orbit, IONEX not used; 240 epochs)

Obs. Length	((09)-(05))	((14)-(05))	((22)-(05))	((30)-(05))
16 min	24045829	-6856446	12167118	-13860004
20 min	24045829	-6856445	12167119	-13860004
32 min	24045829	-6856445	12167119	-13860004
40 min	24045828	-6856447	12167118	-13860004
60 min	24045828	-6856447	12167118	-13860004
120 min	24045828	-6856447	12167118	-13860004

Tab. 7b Estimated baseline length of SpprTmkm
(Obt0Ion0: broadcast orbit, IONEX not used; 240 epochs)

Obs. length	Avg of BL by LI (m)	Sgm of BL by LI (m)	Avg of BL by LW (m)	Sgm of BL by LW (m)
16 min	43382.612	0.007	43382.607	0.007
20 min	43382.704	0.007	43382.610	0.007
32 min	43382.709	0.011	43382.607	0.007
40 min	43382.566	0.006	43382.607	0.006
60 min	43382.568	0.007	43382.611	0.006
120 min	43382.565	0.010	43382.608	0.013

Tab. 8 Accuracy of baseline length measured by using LI (Obt1Ion1: precise orbit, IONEX; Epoch=30 sec)

Baseline	Meas. Length	Correct (040604)	Estimated by LI (m)		Estimated by LW (m)	
			Average	Sigma	Average	Sigma
SpprChts	120 min	23996.2882	23996.295	0.009	23996.292	0.015
SawrHkdm	90 min	33672.0752	33672.083	0.009	33672.052	0.016
SpprTmkm	120 min	43382.5658	43382.570	0.009	43382.588	0.023
TmkmMrrn	120 min	62586.6979	62586.706	0.009	62586.783	0.042
SpprMrrn	120 min	72209.2015	72209.215	0.014	72209.263	0.015
SpprSawar	90 min	107241.9608	107241.973	0.014	107242.043	0.025
SpprHkdm	120 min	134834.1853	134834.195	0.021	134834.247	0.022
HkdmIwa2	120 min	236900.8818	236900.989	0.019	236900.852	0.202
MrrnIwa2	120 min	289582.5476	289582.622	0.013	289582.475	0.202
SpprIwa2	120 min	349369.9159	349369.976	0.007	349369.884	0.198
SpprKsnm	120 min	452359.1513	452359.201	0.014	452359.020	0.220
SpprKtib	120 min	686401.7925	686401.794	0.063	686401.428	0.285
SpprIchk	120 min	818216.6083	818216.529	0.111	818216.191	0.262

The results for SpprTmkm whose baseline length is 43382.566 m are shown in Tables 6 and 7. Te results in Table 6 are obtained by using the precise orbits and the ionospheric delays by IONEX, and those in Table 7 by using the broadcast orbits and by neglecting the ionospheric delays. When the baseline becomes short, the correct results are obtained by using the short observation length. In case of the short baseline length, the correct data are obtained even if the ionospheric delays are neglected. However, the ionospheric data are useful in shortening the observation length.

5 Effects of baseline length on precision of measurements

The effects of the baseline length on the positioning accuracy are shown in Tables 8. As the baseline length becomes longer, the accuracy becomes lower. The results tell that the estimation error is less than 10 cm, even if the baseline length exceeds 200 km.

For reference the results obtained by using the broadcast orbits and neglecting the ionospheric delays are shown in Table 9. For example, in case of SpprIwa2 whose baseline is 350 km, there seem to exist no big difference between the results in Table 8 and those in Table 9. However, if the variations are compared, the results obtained by utilizing the ionospheric delays give the higher precision as shown in Figs. 3a and 3b.

Tab. 9 Accuracy of baseline length measured by using LI (Obt0Ion0: broadcast orbit, IONEX not used; Epoch=30 sec)

Baseline	Meas. Length	Correct (040604)	Estimated by LI (m)		Estimated by LW (m)	
			Average	Sigma	Average	Sigma
SpprChts	120 min	23996.2882	23996.292	0.009	23996.309	0.011
SawrHkdm	90 min	33672.0752	33672.082	0.009	33672.096	0.009
SpprTmkm	120 min	43382.5658	43382.565	0.010	43382.608	0.013
TmkmMrrn	120 min	62586.6979	62586.710	0.011	62586.815	0.034
SpprMrrn	120 min	72209.2015	72209.218	0.016	72209.328	0.017
SpprSawar	90 min	107241.9608	107241.981	0.017	107242.131	0.025
SpprHkdm	120 min	134834.1853	134834.245	0.052	134834.381	0.025
HkdmIwa2	120 min	236900.8818	236900.969	0.018	236901.143	0.114
MrrnIwa2	120 min	289582.5476	289582.609	0.015	289582.846	0.112
SpprIwa2	120 min	349369.9159	349369.976	0.028	349370.329	0.118
SpprKsnm	120 min	452359.1513	452359.224	0.063	452359.671	0.125
SpprKtib	120 min	686401.7925	686401.948	0.140	686402.606	0.141
SpprIchk	120 min	818216.6083	818216.961	0.143	818217.630	0.130

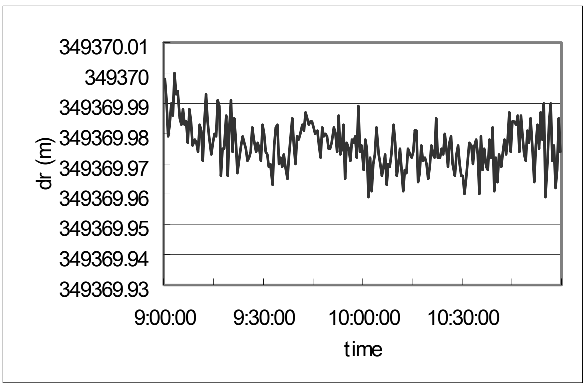

Fig. 3a Baseline length of SpprIwa2 by LI
(Obt1Ion1: precise orbit, IONEX; Epoch=30 sec)

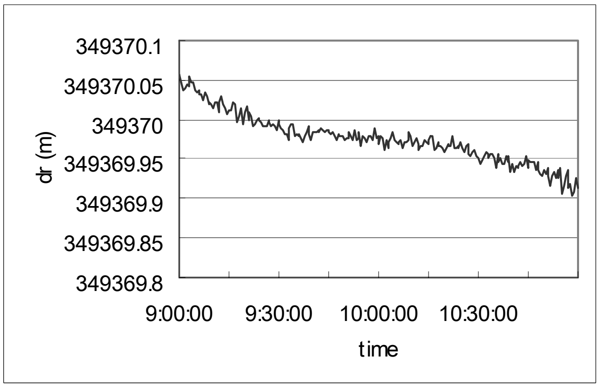

Fig. 3b Baseline length of SpprIwa2 by LI
(Obt0Ion0: broadcast orbit, IONEX not used; Epoch=30 sec)

6 Algorithm for real time processing

The results discussed above were obtained by the offline processing. An algorithm for the real time processing can be made easily. Instead of taking average over the whole epochs, the average is taken over specified epochs in the nearest past. An algorithm is shown in Fig. 4. Kalman filters may also be used instead of taking average over the past epochs. For the estimation of the LW ambiguity

$N_{W12\alpha\beta}^{ij}$, a Kalman filter may be effectively used, where $N_{W12\alpha\beta}^{ij}$, Eq. (3) and the constant nature of $N_{W12\alpha\beta}^{ij}$ are the state variable, observation equation and system transition equation.

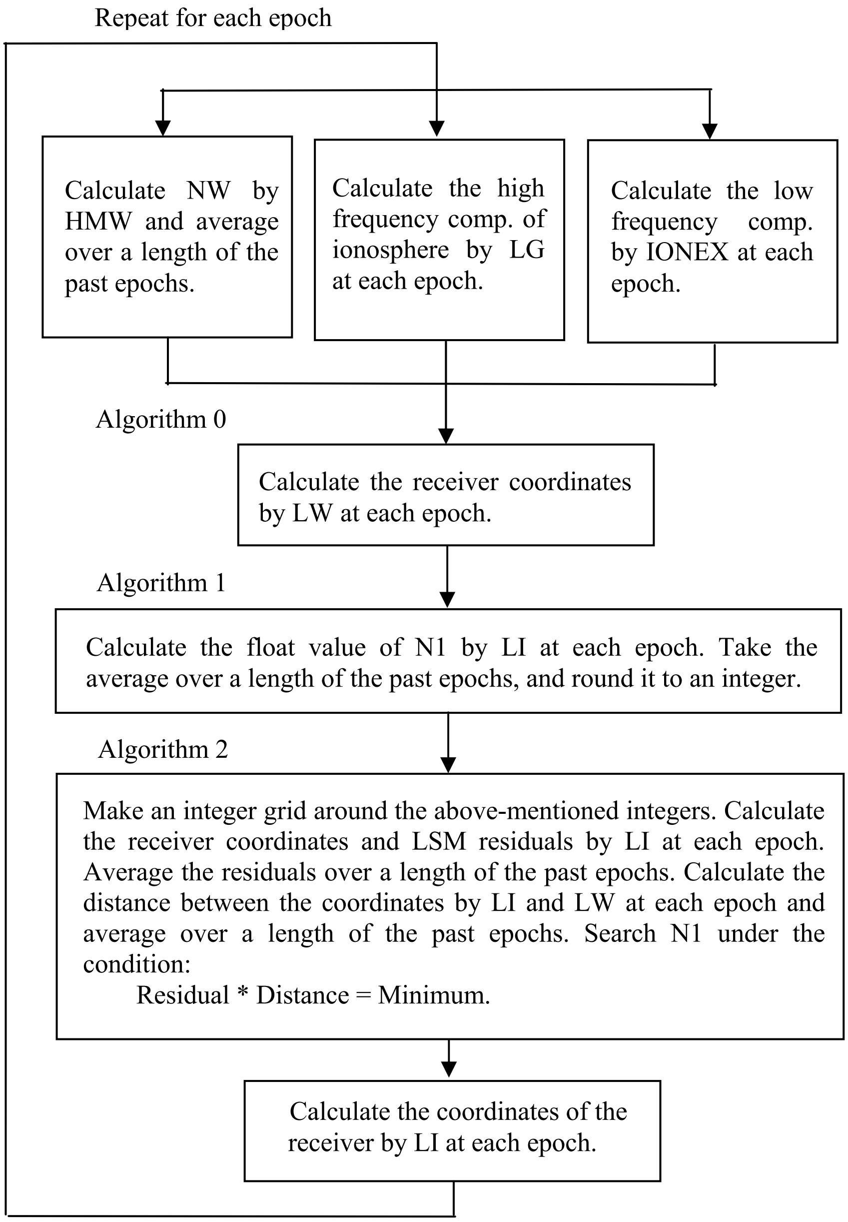

Fig. 4 Algorithm for positioning (Real-time algorithm)

7 Epoch interval of a base station

The epoch interval of the GEONET data downloaded from the homepage of GSI at free of charge is 30 seconds. On the other hand, that of the kinematic positioning is usually 1 second. It may be very useful, if the kinematic positioning of 1 second epoch is possible by combining the rover data of 1 second epoch with the base data of 30 second epoch supplied by GEONET. Furthermore, the merits in the data saving and transmission may be big, if the epoch interval of the base station data can be taken long.

Since the base station is fixed, it does not make unpredictable motions. The ionospheric and tropospheric delays may make small changes within 30 seconds and may be assumed continuous. So, errors included in the 1-second epoch data generated by interpolation of the 30-second epoch data may be small.

In the following numerical examples, the epoch interval of the rover is 5 seconds. Fourth order polynomials are obtained by using Least Square Fitting of nine point data of 30 second epoch. Assuming the offline or real time processing, the data of 5 second epoch are generated by interpolation or extrapolation by using the polynomials.

Figs. 5 and 6 show comparisons of the baseline length calculated by using the raw data with that by the interpolated and extrapolated data respectively. In case of the interpolation, the difference is small, about one centimeter. The difference in case of the extrapolation is bigger, several centimeters. The efforts to lessen the error of the extrapolation should be made.

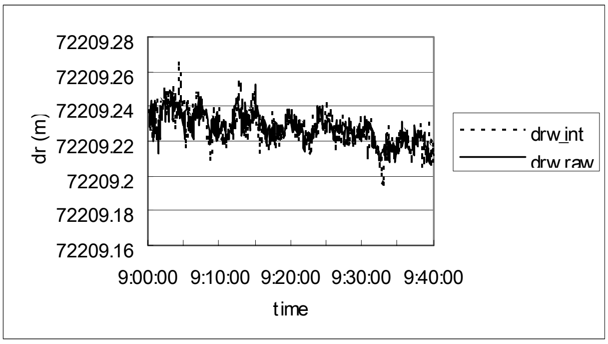

Fig. 5 Baseline length of SpprTmkm obtained by LI, where base station data are generated by interpolation (2004.06.04)

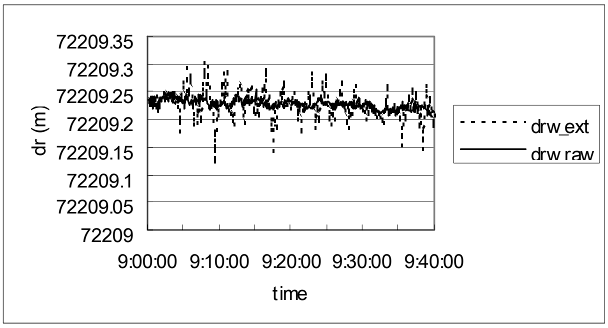

Fig. 6 Baseline length of SpprTmkm obtained by LI, where base station data are generated by extrapolation (2004.06.04)

8 Conclusion

In the previous report (Isshiki, 2004b), a new theory and algorithm of the dual frequency long baseline kinematic positioning were discussed, and the validity was proved by conducting some numerical calculations using the observation data of 30 sec in epoch interval. According to this new solution, the rather precise kinematic positioning was possible for the baseline whose length is several hundred kilometers.

In the present report, the effects of the epoch interval and the observation length are studied by using the observation data of 1 sec in epoch interval. As a result, it was clarified that the long enough observation length is required for the accurate positioning, and the epoch interval itself is not so important. However, the necessary observation length is a function of the baseline length and the ionospheric delays. In order to make this solution useful in practical applications, more data should be analyzed, and a guideline on this point should be given.

The relationship between the baseline length and the positioning error is also investigated. And it was confirmed that a rather accurate positioning is possible by the present solution for the baseline whose length is several hundred kilometers.

An algorithm for the real time positioning is also shown.

Acknowledgements

Nippon GPS Data Service supplied the observation data of one second in epoch interval with cooperation of Mr. M. Kanzaki of Nippon GPS Solutions Corporation. It was very helpful for the verification of the algorithm to be able to select freely the observation stations in GEONET. The author would like to express his sincere thanks to Mr. Kanzaki and both companies.

References

Isshiki H. (2003a): ***An application of wide-lane to long baseline GPS measurements (3)***, ION GPS/GNSS 2003, The Institute of Navigation

Isshiki H. (2003b): ***An approach to ambiguity resolution in multi frequency kinematic positioning***, Proceedings of 2003 International Symposium on GPS/GNSS, pp. 545-552

Isshiki,H. (2003c): ***Long baseline technology for floating body motion measurements in ocean by GPS –Possibility of dual frequency system–***, Conference Proceedings The Society of Naval Architects of Japan, Vol. 2 No.2003A-GS2-2, in Japanese

Isshiki H. (2004a): ***Long baseline GPS kinematic positioning by wide-lane combination***, Conference Proceedings The Society of Naval Architects of Japan, Vol. 3 No.2004S-G2-10, in Japanese.

Isshiki H. (2004b): ***A long baseline kinematic GPS solution of ionosphere-free combination constrained by widelane combination***, OCEANS'04, Kobe, Japan

Hatch R. (1982): ***Synergism of GPS code and carrier measurements***, Proceedings of the Third International Geodetic Symposium on Satellite Doppler Positioning, New Mexico State University, pp.1213-1232

Melbourne W. G. (1985): ***The case for ranging in GPS based geodetic systems***, Proceedings 1st International Symposium on Precise Positioning with the Global

Positioning System, edited by Clyde Goad, pp. 403-412, U. S. Department of Commerce, Rockville, Maryland

Wübbena G. (1985): ***Software developments for geodetic positioning with GPS using TI 4100 code and carrier measurements***, Proceedings 1st International Symp. on Precise Positioning with the Global Positioning System, edited by Clyde Goad, pp. 403-412, U. S. Dept. of Commerce, Rockville, Maryland

Hugeltobler H.; Schaer S.; Fridez P. (2001): *Bernese GPS Software Version 4.2*, Astronomical Institute, University of Berne